

Gravin Is a Transitory Effector of Polo-like Kinase 1 during Cell Division

David A. Canton,^{1,2} C. Dirk Keene,³ Katie Swinney,² Lorene K. Langeberg,^{1,2} Vivian Nguyen,⁶ Laurence Pelletier,⁶ Tony Pawson,⁶ Linda Wordeman,⁴ Nephi Stella,^{2,5} and John D. Scott^{1,2,*}

¹Howard Hughes Medical Institute

²Department of Pharmacology

³Department of Pathology, Neuropathology Division

⁴Department of Physiology and Biophysics

⁵Psychiatry and Behavioral Sciences

University of Washington, Seattle, WA 98195, USA

⁶Samuel Lunenfeld Research Institute, Mount Sinai Hospital, Joseph and Wolf Lebovic Health Complex, Toronto, ON M5G 1X5, Canada

*Correspondence: scottjd@uw.edu

<http://dx.doi.org/10.1016/j.molcel.2012.09.002>

SUMMARY

The mitogenic and second-messenger signals that promote cell proliferation often proceed through multienzyme complexes. The kinase-anchoring protein Gravin integrates cAMP and calcium/phospholipid signals at the plasma membrane by sequestering protein kinases A and C with G protein-coupled receptors. In this report we define a role for Gravin as a temporal organizer of phosphorylation-dependent protein-protein interactions during mitosis. Mass spectrometry, molecular, and cellular approaches show that CDK1/Cyclin B1 phosphorylates Gravin on threonine 766 to prime the recruitment of the polo-like kinase Plk1 at defined phases of mitosis. Fluorescent live-cell imaging reveals that cells depleted of Gravin exhibit mitotic defects that include protracted prometaphase and misalignment of chromosomes. Moreover, a Gravin T766A phosphosite mutant that is unable to interact with Plk1 negatively impacts cell proliferation. In situ detection of phospho-T766 Gravin in biopsy sections of human glioblastomas suggests that this phosphorylation event might identify malignant neoplasms.

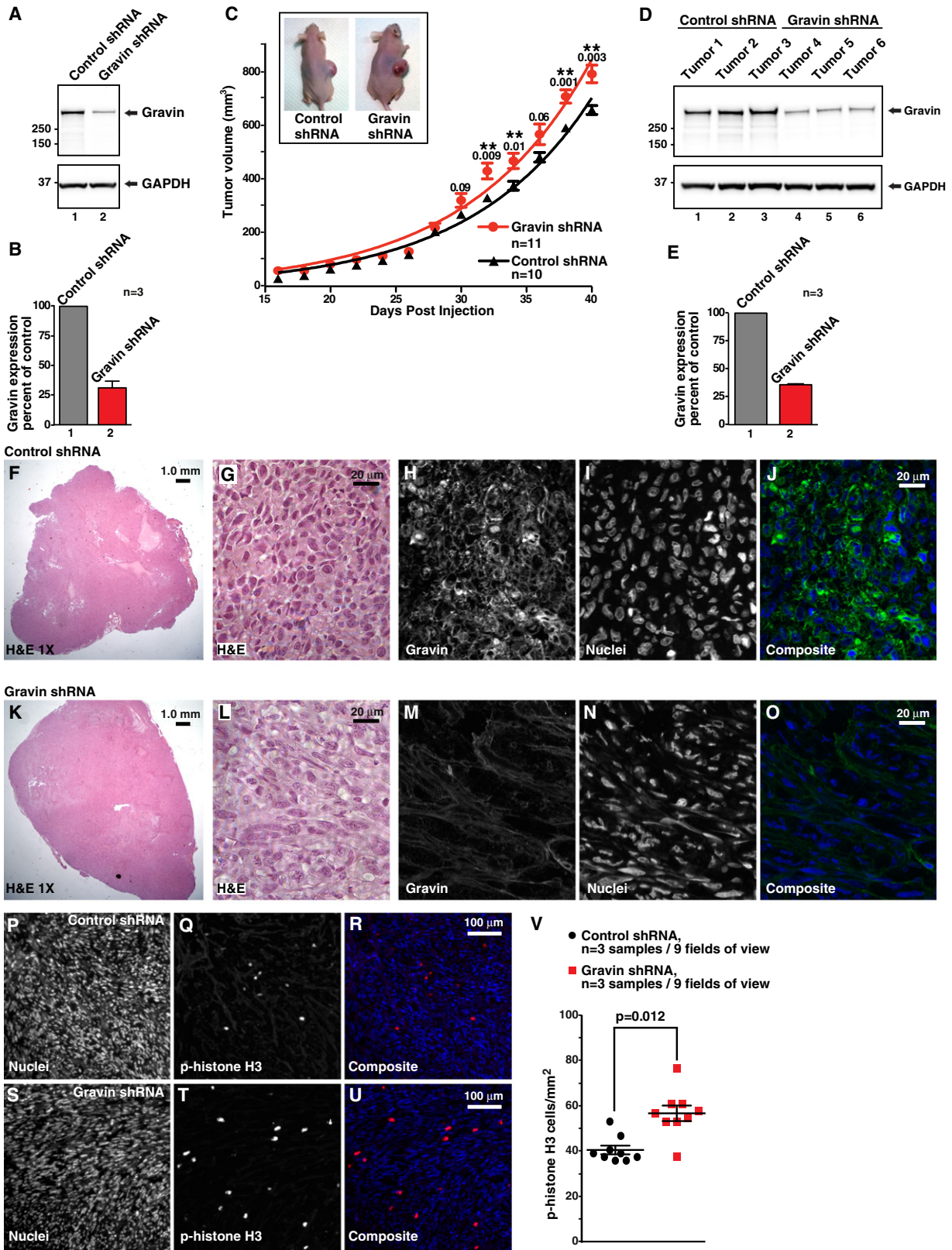
INTRODUCTION

Signal transduction cascades transfer information from environmental cues to intracellular effectors. This dynamic process requires the diffusion of chemical signals or ions through the cytoplasm to sites where they are processed by multienzyme complexes (Scott and Pawson, 2009). The linear transfer of information through mitogen-activated protein (MAP) kinase cascades epitomizes this process. Scaffolding proteins provide structural integrity to these three-tier kinase cascades by organizing and orienting their enzyme-binding partners to ensure

that the terminal MAP kinase encounters a subset of downstream targets to initiate cell division (Ahn, 2009; Morrison and Davis, 2003; Smith et al., 2010). Prototypic examples of mammalian scaffolding proteins include kinase suppressor of Ras (KSR), which organizes the Raf/MEK/ERK kinase cascades and Jun-interacting proteins (JIPs) that synchronize enzymes in the Jun N-terminal kinase cascade (Dougherty et al., 2009; Nihalani et al., 2001). Scaffold proteins such as 14-3-3 coordinate cell division through the control of mitotic entry and cytokinesis (Gardino and Yaffe, 2011).

An emerging concept in drug discovery is the realization that kinase scaffolds represent unique therapeutic targets (Hoshi et al., 2010). Likewise, the development of anticancer drugs that inhibit cell-cycle protein kinases is a frontier in therapeutic intervention (Fabbro et al., 2012). One promising target is the polo-like serine/threonine kinase Plk1, an enzyme that is induced as cells enter mitosis to sustain spindle assembly and that accumulates to supraphysiological levels in several cancers (Christoph and Schuler, 2011). As a result, small-molecule inhibitors such as BI2536 or GW843682 should preferentially target Plk1 at distinct phases of mitosis (Strebhardt and Ullrich, 2006). However, a biological property of this kinase that limits the efficacy of these compounds is that Plk1 continually changes its subcellular location throughout the cell cycle. Hence it is imperative to ascertain how Plk1 anchoring is managed in dividing cells and malignant tumors. In this report we define a role for the scaffolding protein Gravin as a transitory effector of Plk1 during mitosis.

Gravin was discovered as an autoantigen in serum from patients with myasthenia gravis (Gordon et al., 1992). Subsequent analyses revealed that Gravin synchronizes second-messenger-regulated events by associating with the β_2 -adrenergic receptor and sequestering protein kinases A and C in proximity with cAMP phosphodiesterases and substrates (Nauert et al., 1997; Tao et al., 2003; Willoughby et al., 2006). The rodent ortholog, SSeCKS, sequesters cyclins and is downregulated in Src-transformed fibroblasts (Lin and Gelman, 1997). Here we show that transient phosphorylation of Gravin by CDK1/Cyclin B1 elicits the recruitment of Plk1 to ensure efficient mitotic progression.



RESULTS

Depletion of Gravin Increases Tumor Size

Chromosome instability derived from aberrant cell division drives cancers to a state of aneuploidy. Aneuploidy, in turn, promotes mutations that lead to tumorigenesis (Kolodner et al., 2011). The human kinase anchoring protein Gravin/AKAP12 is postulated to play a role in cellular transformation, but the molecular details of this mechanism have not been established (Gelman, 2010). Therefore, we evaluated the contribution of Gravin to tumor growth in immunodeficient mice. As a prelude to these studies, human U251 glioma cells were infected with lentivirus encoding a small hairpin RNA (shRNA) targeting Gravin. Gravin protein levels were reduced by $68.5\% \pm 3.2\%$ ($n = 3 \pm \text{SEM}$) compared to cells harboring a control shRNA as assessed by immunoblot (Figure 1A, top panel, and Figure 1B). GAPDH served as a loading control (Figure 1A, bottom panel). Next, U251 cells stably expressing the shRNAs were implanted subcutaneously into the flanks of athymic Nu/J mice (Figure 1C and see Figures S1A and S1B online). Tumor volume was monitored from 16 to 40 days postinjection. Depletion of Gravin resulted in a small but discernable increase in tumor growth (Figure 1C, control shRNA, $n = 10$; Gravin shRNA, $n = 11$; $**p \leq 0.05$).

Gravin gene silencing in these tumors was assessed by two independent methods (Figures 1D–1O). First, immunoblot analysis of extracts from randomly selected tumors measured a $64.1\% \pm 0.5\%$ ($n = 3 \pm \text{SEM}$) decrease in Gravin protein compared to controls (Figure 1D, top panel, lanes 4–6, and Figure 1E). GAPDH served as a loading control (Figure 1D, bottom panel). Second, hematoxylin and eosin staining (H&E) of paraffin-embedded tumor sections did not reveal striking morphological differences between the control and Gravin-depleted tissues (Figures 1F and 1G, control shRNA; and Figures 1K and 1L, Gravin shRNA). Immunofluorescent staining confirmed gene silencing of Gravin (Figures 1H–1J and Figures 1M–1O). Staining with DRAQ5 served as a nuclear marker (Figures 1I and 1N). Tumor sections were stained for phosphoserine10 Histone H3, a mitotic cell marker, to look for changes in cell proliferation. Phospho-H3-positive cells were monitored in $800 \mu\text{m}^2$ sectors of selected tumors (Figures 1P–1U). Gene silencing of Gravin promotes a 25.77% increase in phospho-H3-positive cells (Figure 1V, represents $n = 3 \pm \text{SEM}$). Thus, the amalgamated data in Figure 1 infer that Gravin contributes to the fidelity of cell-cycle progression but has little effect on tumor growth.

Gravin Is Phosphorylated by CDK1/Cyclin B1

We hypothesized that increased detection of phosphohistone H3 and subtle changes in tumor volume following Gravin knock-

down were emblematic of delayed mitotic progression. Therefore, we first investigated phosphorylation of Gravin by the principle mitotic kinase CDK1 (Enserink and Kolodner, 2010). Experiments were conducted in three phases. Initially, bioinformatic searches using the Scansite algorithm (Obenauer et al., 2003) predicted CDK1 phosphorylation sites at Ser513, Thr617, and Thr766. These residues were mutated to alanine in the context of Flag-tagged Gravin and expressed in HEK293 cells. Flag immune complexes were collected and incubated with CDK1/Cyclin B1 in the presence of $\gamma\text{-}^{32}\text{P}\text{-ATP}$. Samples were separated by SDS-PAGE, and ^{32}P incorporation was assessed by autoradiography. Loss of S513, T617, or T766 minimally reduced ^{32}P incorporation compared to wild-type Gravin (Figure 2A, top panel, lanes 2–5, and Figure 2B, gray). However, more pronounced reductions in ^{32}P incorporation were evident upon double mutation of T617 and T766, and replacement of all three putative substrate sites (Figure 2A, lanes 6 and 7; 48% and 92% decrease, respectively; Figure 2B, blue and red, represents $n = 3 \pm \text{SEM}$). Thus, CDK1 can phosphorylate Gravin in vitro.

Next we tested if endogenous Gravin was a target for CDKs in intact cells. HEK293 cells arrested in mitosis with nocodazole were incubated with ^{32}P orthophosphate (Figure 2C). Phosphate incorporation into Gravin immune complexes was evaluated by autoradiography. A robust signal was detected at 300 kDa, the molecular weight of Gravin (Figure 2C, lane 2). Treatment with the selective CDK inhibitor, roscovitine, reduced ^{32}P incorporation by 44% (Figure 2C, lane 3; Figure 2D quantitation represents $n = 3 \pm \text{SEM}$).

A more stringent second phase of analyses employed mass spectrometry to globally identify sites of mitotic phosphorylation on Gravin. Nineteen phosphorylation sites were assigned (Figure 2E, left column), of which ten were lost following roscovitine treatment (Figure 2E, Figure S2A, and Table S1). Within this subset, only the S513, T617, and T766 sites conformed to the canonical CDK1 consensus sequence -S/T-P-X-K/R-K (Alexander et al., 2011; Figures 2E and 2F). Since the T766 site is strictly conserved across species (Figure 2G), the third phase of analysis was implemented to generate a phospho-specific antibody. This reagent was used as a tool to evaluate the biology of the Thr766 phosphorylation event.

Five complimentary approaches characterized the affinity-purified phospho-T766 Gravin antisera. First, analysis of peptide spot arrays confirmed that the antisera recognized the immobilized target phosphopeptide antigen but was refractory to peptide variants that incorporated threonine or alanine at position 766 (Figure 2H). Second, the phospho-T766 antiserum detected Gravin from mitotic cells but was unable to react with

Figure 1. Gravin Suppresses Tumor Growth

(A) Immunoblot analysis of U251 cells stably expressing control (lane 1) or Gravin shRNA (lane 2). Staining with antibodies against Gravin (top) and GAPDH (bottom). (B) Densitometric analyses of amalgamated data ($n = 3 \pm \text{SEM}$) normalized to GAPDH. (C) Stable U251 cells (3×10^6) were injected into the rear flank of athymic (NU/J) mice. Tumor volume was measured 16–40 days postinjection (black, control shRNA $n = 10 \pm \text{SEM}$; red, Gravin shRNA, $n = 11 \pm \text{SEM}$; $**p \leq 0.05$). (D) Immunoblot analysis of tumor extracts (indicated above each lane) with antibodies against Gravin (top) and GAPDH (bottom). (E) Densitometric analyses of amalgamated data ($n = 3 \pm \text{SEM}$). The morphology of paraffin-embedded sections of tumor (F, G, K, and L) was evaluated by H&E staining. Serial sections (H–J, N, and O) costained with anti-Gravin (green) and DRAQ5 (blue) as a nuclear marker confirmed gene silencing of Gravin in situ. (P–R and S–U) Phospho-Histone H3 staining of mitotic cells within the tumor (red). (V) Graph depicting the numbers of phospho-Histone H3-positive cells (per mm^2) in control (black) and Gravin shRNA (red) tumor sections ($n = 3$ individual tumors $\pm \text{SEM}$; $p = 0.012$).

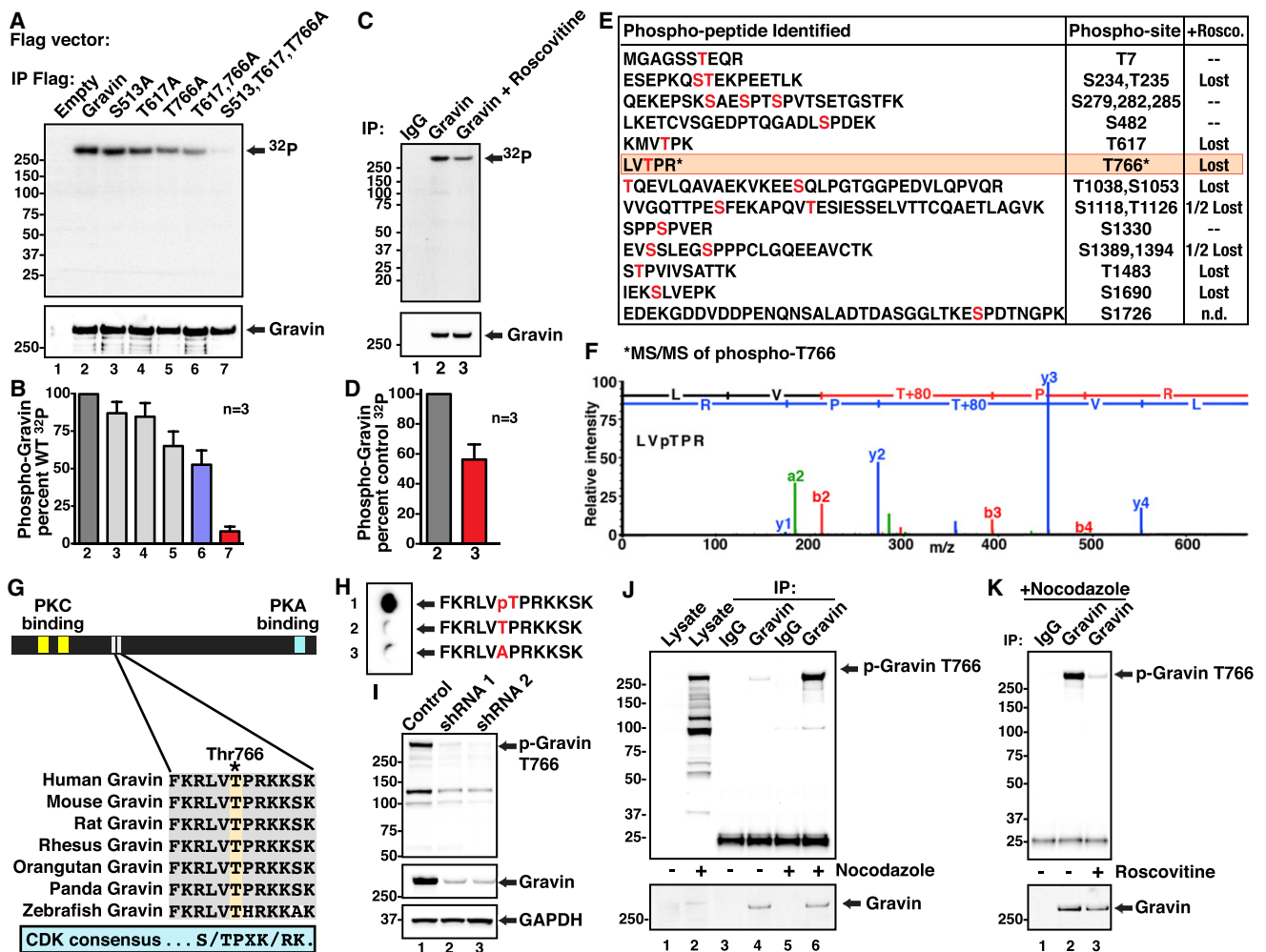


Figure 2. Gravin Is Phosphorylated by CDK1/Cyclin B

Consensus CDK-phosphorylation sites were disrupted by replacing the target serine or threonine with alanine. (A) Gravin mutants (indicated above each lane) were expressed in HEK293 cells. Immunokinase assays were performed on the Flag pull-downs using exogenous CDK1/Cyclin B1 and γ -³²P ATP. (B) Quantitation of autoradiographs (n = 3 ± SEM). (C) HEK293 cells were arrested in mitosis with nocodazole (0.1 μg/mL) and treated with the CDK-inhibitor roscovitine (75 μM) in the presence of ³²P ortho-phosphate. Gravin was immunoprecipitated and detected by autoradiography (top) and anti-Gravin immunoblot (bottom). (D) Quantitation of autoradiographs (n = 3 ± SEM). (E) Mass spectrometry analysis of Gravin phosphorylation in vivo; (left panel) all phospho-peptides assigned; (middle panel) phosphosite (human amino acid numbering); (right panel) sites lost upon roscovitine treatment are indicated. (F) Spectral trace of the sequence surrounding phosphothreonine 766. (G) Sequence conservation of threonine 766 (species are indicated). (H) Characterization of phospho-T766 Gravin antiserum on peptide spot arrays (sequences of peptide derivatives are indicated). (I) Gravin was depleted from HEK293 cells with two independent shRNAs. Cell lysates were immunoblotted with antibodies against phospho-T766 Gravin (top), Gravin (middle), and GAPDH (bottom) as a loading control. (J) Gravin was immunoprecipitated from control HEK293 cells or cells arrested in mitosis with nocodazole. Immunoblot detection of phospho-T766 Gravin (top) or Gravin (bottom) is shown. (K) HEK293 cells were arrested in mitosis in the absence (lanes 1 and 2) or presence (lane 3) of roscovitine. Immunoblot detection of phospho-T766 Gravin (top) or Gravin (bottom) in immune complexes is shown.

the Gravin T766A mutant (Figure S2B). Third, depletion of Gravin from mitotic HEK293 cells using two independent shRNAs abolished detection of the phospho-T766 signal as assessed by immunoblot (Figure 2I, top panel). Note that Gravin knock-down also reduced the detection of lower molecular weight

bands that likely represent degradation products of the scaffolding protein. Fourth, we examined phosphorylation of endogenous Gravin in cycling versus mitotic cells. Only lysates from mitotic cells showed specific reactivity with the anti-phospho-T766 Gravin antisera (Figure 2J, top panel, lanes 1 and 2).

Moreover, only Gravin immunoprecipitated from mitotic cells was recognized by the phosphoantibody compared to IgG controls (Figure 2J, top panel, lanes 5 and 6). No reactivity was detected if Gravin was immunoprecipitated from cycling cells (Figure 2J, lanes 3 and 4). Lastly, inhibition of CDKs in mitotic cells with roscovitine blocked the phospho-T766 Gravin signal (Figure 2K, top panel). Thus, data in Figure 2 argue that CDK phosphorylates Gravin at multiple sites and that our antibody specifically recognizes Gravin when phosphorylated on Thr766.

T766 Phosphorylation during Mitosis

Our working hypothesis was that the phosphorylation state of T766 on Gravin changes through the cell cycle. To test this notion, HEK293 cells arrested at the G1/S boundary by double thymidine block were released into fresh media, and the phosphorylation state of Gravin was analyzed every 2 hr by immunoblot (Figure 3A). Threonine 766 phosphorylation on Gravin peaked at 12 hr postrelease and occurred concurrently with phosphorylation of serine 10 on Histone H3 as cells entered mitosis (Figure 3A, panels 1 and 3). Gravin protein levels were constant throughout the time course of the experiment (Figure 3A, panel 2), and the amalgamated densitometry data further confirmed these results (Figure 3B; $n = 3 \pm \text{SEM}$, normalized to GAPDH loading control). Analysis of additional cell-cycle marker proteins validated our findings (Figure 3C). As expected, expression of the mitotic kinase Plk1 and its priming phosphorylation on threonine 210 peaked during mitosis, along with levels of Cyclin B1 (Figure 3C, panels 1–3). Conversely, the inhibitory kinase Wee1 was elevated at the G1/S boundary and declined as cells entered mitosis (Figure 3C, panel 4). The inhibitory phosphorylation of CDK1 on tyrosine 15 was lost as cells progressed toward division (Figure 3C, panel 5). Similar results were found in cells released from the thymidine block and trapped in mitosis with nocodazole (Figures S3A and S3B). Thus, phosphorylation of T766 on Gravin is a temporally regulated mitotic event.

This notion was further substantiated *in situ* by immunofluorescence detection of phospho-T766 Gravin in cells at different stages of the cell cycle (Figures 3D–3W). During interphase, Gravin (green) decorated the plasma membrane and appeared as punctate staining throughout the cell (Figure 3D). The phospho-T766 Gravin signal (red) was barely detectable, and DRAQ5 (blue) was used as a DNA marker (Figures 3E–3G). At prophase, phospho-T766 Gravin was evident in the nucleus, while total Gravin was evenly distributed throughout the cytosol (Figures 3H–3K). Upon formation of the metaphase plate, the total and phospho-T766 Gravin signals aligned on the centrosomes and at the spindle poles (Figures 3L–3O). In anaphase (Figures 3P–3S) and telophase (Figures 3T–3W), phospho-T766 staining was restricted to the centrosomes, while total Gravin exhibited a punctate staining pattern throughout the cytosol. Collectively, data in Figure 3 indicate that Gravin, when phosphorylated on threonine 766, concentrates at the centrosomes and mitotic spindle in dividing cells.

Gravin Interacts with the Mitotic Kinase Plk1

Independent confirmation of the above result was provided by analysis of mitotic spindle fractions prepared using a published

method (Silljé and Nigg, 2006). The quality of each preparation was validated by immunoblot detection of the marker proteins pericentriolar material-1 (PCM-1) and α -tubulin (Figure 4A, left side, upper panels). Additional quality-control immunoblots confirmed that actin and GAPDH were absent in the spindle preparations (Figure 4A, left side, bottom panels). The majority of Gravin was detected in total cell lysates (Figure 4A, right top panel), whereas phospho-T766 Gravin pool was enriched in the spindle fraction (Figure 4A, right middle panel). Notably, polo-like kinase 1 (Plk1), an enzyme that associates with centrosomes and mitotic spindle (Petronczki et al., 2008), was enriched in this fraction (Figure 4A, right bottom panel).

We noticed that the residues surrounding T766 on Gravin (-LVpTPPR-) resemble a canonical Plk1-binding site (Elia et al., 2003). Since this mitotic kinase interacts with binding partners in a phosphorylation-dependent manner, we tested whether Plk1 activity copurifies with T766-phosphorylated Gravin. Gravin or phospho-T766 Gravin immune complexes from solubilized mitotic spindle preps were screened for copurification of Plk1 activity using the selective substrate peptide ISDELMDATFAD QEAKKK (Bain et al., 2007). Background levels of Plk1 activity were present in total Gravin immunoprecipitations (Figure 4B, columns 1 and 3), whereas 46.6% \pm 9.1% ($n = 3 \pm \text{SEM}$) of the available kinase activity was detected in phospho-T766 Gravin immune complexes (Figure 4B, columns 2 and 4). Control immunoblots confirmed that Plk1 copurified with phospho-T766 Gravin (Figure 4B, lower panel, lane 4). These results demonstrate that active Plk1 associates with phospho-T766 Gravin in the mitotic spindle preparation.

The above studies were verified by testing if ectopically expressed Gravin and Plk1 copurify from mitotic cell lysates. HEK293 cells overexpressing Plk1-V5 and GFP-Gravin were arrested in mitosis with nocodazole. Immunoblot analyses revealed that Plk1-V5 copurified with Gravin-GFP immune complexes, but not with GFP alone (Figure 4C). Reciprocal experiments confirmed that Gravin-GFP was present in Plk1-V5 immune complexes, but not controls (Figure 4D). More stringent analyses established that endogenous Gravin cofractionated with Plk1 (Figure 4E, lane 6). In contrast, Gravin-Plk1 complexes were not detected in cycling HEK293 cells (Figure 4E, lane 4). These findings were reproduced in HeLa cells (Figure S4A). Thus, Gravin interacts with Plk1 during mitosis, validating a proteomic screen that identified the anchoring protein as one of 622 polo-box-interacting proteins (Lowery et al., 2007).

The spatial and temporal pattern of Gravin-Plk1 interplay was imaged at defined phases of the cell cycle (Figures 4F–4Y). At interphase, Plk1 (green) and phospho-T766 Gravin (red) were hardly detected (Figures 4F–4I). Yet, as cells entered prophase, the Plk1 and phospho-T766 Gravin staining was detected in the nuclei and intermingled with the DNA marker DRAQ5 (blue, Figures 4J–4M). By metaphase, Plk1 and phospho-T766 Gravin were concentrated at the spindle poles, but Plk1 additionally stained the kinetochore (Figures 4N–4Q). In anaphase, Plk1 migrated to the spindle midzone, whereas the phospho-T766 Gravin signal was detected on the centrosomes (Figures 4R–4U). The spatial segregation of both proteins was more evident during telophase and cytokinesis when Plk1 congregated at the midbody, adjacent to the cytokinetic ring separating the

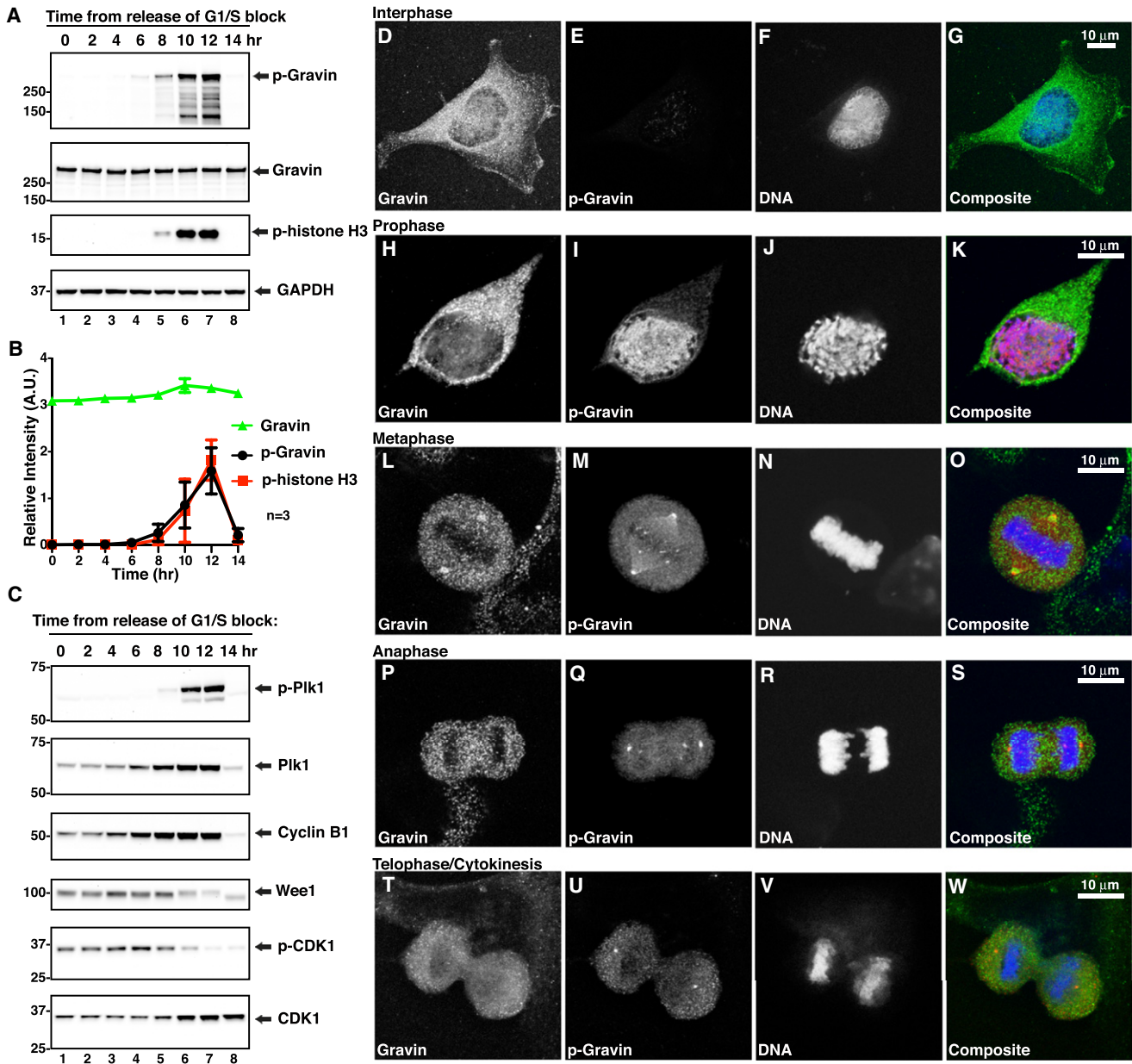


Figure 3. Phosphorylation of Gravin at Threonine 766 during Mitosis

(A) HEK293 cells were arrested at the G1/S boundary by double thymidine block. Cells were released from the block and harvested every 2 hr from time 0 to 14 (indicated above each lane). Immunoblot detection of phospho-T766 Gravin (top), Gravin (middle) and phospho-S10 Histone H3 (bottom) in cell extracts.

(B) Quantitation represents data normalized to GAPDH loading control (phospho-T766 Gravin black trace, phospho-Histone H3 red, Gravin green; $n = 3 \pm \text{SEM}$).

(C) Immunoblot detection of additional cell-cycle markers as indicated.

(D–W) HEK293 cells grown on coverslips were synchronized by double thymidine block, released into fresh media, and fixed in ice-cold methanol 8–9 hr later. Immunofluorescence of cells at defined stages of the cell cycle was performed with antibodies as indicated, followed by detection with secondary antibodies conjugated to Alexa Fluor dyes.

emerging daughter cells (Figures 4V–4Y). Similar patterns for Plk1 and phospho-T766 Gravin staining were observed when immunofluorescence experiments were repeated in mitotic Rat-2 fibroblasts (Figures S4B–S4Y). Taken together, the data in Figure 4 demonstrate that phospho-T766 Gravin and Plk1 copurify on mitotic spindles and interact at defined phases of mitosis.

Gravin-Plk1 Interaction Facilitates Cell-Cycle Progression

Plk1 interacts with its binding partners through its polo-box domain (PBD; Elia et al., 2003). CDK1 is frequently responsible for a priming phosphorylation on the PBD-interacting protein, such as the sequence surrounding Thr766 on Gravin, although

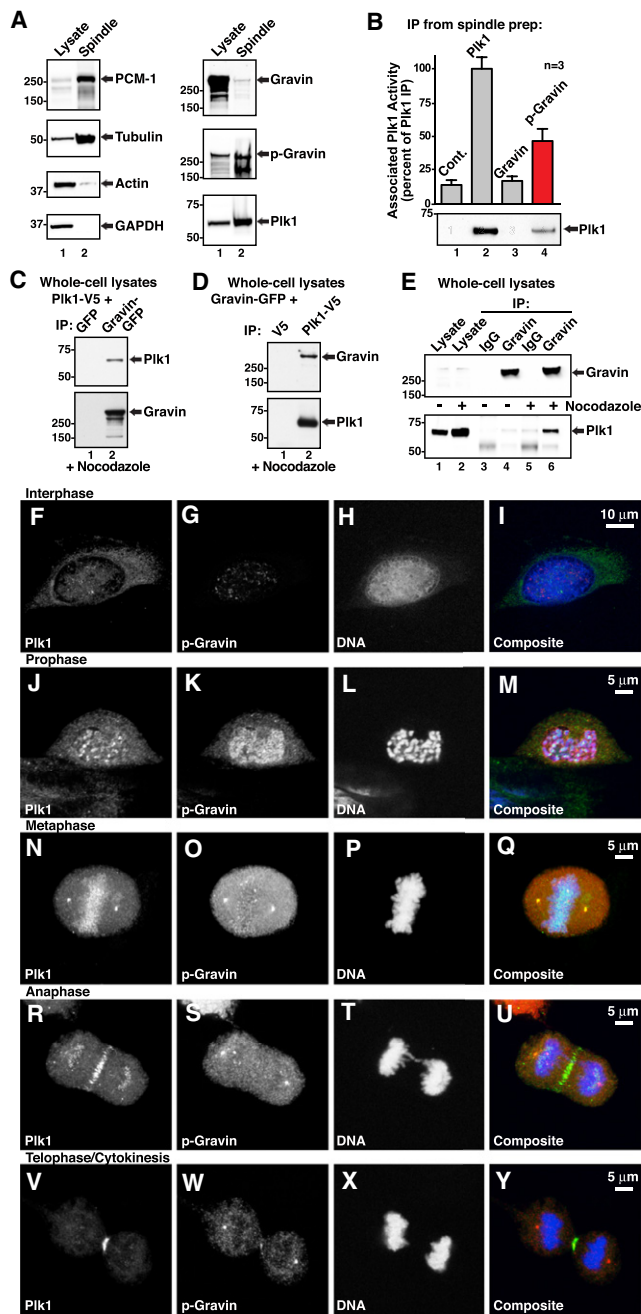


Figure 4. Phospho-T766 Gravin Recruits the Mitotic Kinase Plk1

(A) Spindles were isolated from mitotic cells (Silljé and Nigg, 2006), resuspended in sample buffer, and immunoblotted with specific antibodies as indicated.

(B) Mitotic spindles solubilized in lysis buffer were immunoprecipitated with antibodies against Plk1, Gravin, or phospho-T766 Gravin. Immune complexes were subjected to an immunokinase assay using the Plk1 selective peptide -ISDELMDATFADQEAKKK- in the presence of γ - 32 P-ATP. The relative levels of Plk1 activity are indicated.

(C) HEK293 cells were transfected with Plk1-V5 and Gravin-GFP or GFP alone. Copurification of Plk1-V5 (top) and Gravin (bottom) was confirmed by immunoblot.

(D) Reciprocal experiments detected copurification of GFP-Gravin (top) in Plk1-V5 (bottom) immune complexes.

other kinases including Plk1 can perform this function (Lee et al., 2008). To test this hypothesis, immobilized Gravin immune complexes isolated from mitotic HEK293 cell lysates were incubated with a bacterially expressed Plk1 fragment encoding the PBD. Recruitment of the PBD to Gravin was assayed by immunoblot. Preliminary analyses established that PBD binding to Gravin was detectable over IgG controls (Figure 5A, bottom panel, lanes 2 and 3). Dephosphorylation of Gravin with calf intestinal phosphatase abolished PBD binding (Figure 5A, bottom panel, lane 4). Next, selective pharmacological inhibitors were used to identify the “Gravin-priming kinase.” Inhibition of Gravin-associated PKA or PKC with H89 and bisindolylmaleimide 1, respectively, had little effect on PBD binding (Figure 5A, bottom panel, lanes 5 and 7). In contrast, inhibition of CDK1 with roscovitine or Plk1 with GW843682 strongly diminished PBD binding (Figure 5A, bottom panel, lanes 6 and 8). Quantitation of amalgamated data from three independent experiments is presented (Figure 5B).

In order to differentiate between CDK1 and Plk1 priming, we phosphorylated the immunoprecipitated anchoring protein with either purified recombinant kinase. Background levels of PBD binding were detected upon Plk1 phosphorylation and in controls (Figure 5C, bottom panel, lanes 2–4, and Figure 5D). Conversely, incubation with CDK1 resulted in a 3.9-fold ($n = 3$) enrichment of PBD binding to Gravin above basal levels (Figure 5C, bottom panel, lane 5; and Figure 5D). Parallel studies performed with a mutant of the PBD (H538A, K540M) that disrupts interaction with target peptides (Elia et al., 2003) abolished all binding to Gravin (Figures S5A and S5B). Loading controls confirmed equal levels of wild-type and mutant PBDs in all experiments (Figure S5C). Thus, phosphorylation by CDK1 is sufficient to prime Gravin for interaction with Plk1.

Next we asked which CDK1 phosphorylation site on Gravin enhanced PBD binding. Flag-tagged Gravin or individual phosphosite mutants (S513A, T617A, or T766A) were immunoprecipitated from mitotic cell lysates and incubated with a recombinant PBD. PBD binding was assessed by immunoblot (Figure 5E). Loss of S513 or T617 in the context of full-length Gravin did not affect binding to the PBD (Figure 5E, lanes 5 and 6). In contrast, the PBD fragment was unable to bind to the Gravin T766A mutant (Figure 5E, lane 7, and Figure 5F, $n = 3$). Analysis of additional phosphosite mutants confirmed this result (Figure S5D). More mechanistic studies evaluated the effects of introducing aspartic and glutamic acid residues in place of T766. These mutations failed to mimic the role of phosphorylation on Plk1 binding, suggesting a requirement for authentic phosphorylation (Figure S5E). Thus, CDK1 phosphorylation of T766 on Gravin primes the recruitment of Plk1 to this site on the scaffolding protein.

(E) Immunoblot detection of endogenous Gravin (top) and copurification of Plk1 (bottom) from HEK293 cells. Experiments with control (mIgG) antibodies are included.

(F–Y) HEK293 cells on coverslips were synchronized by double thymidine block, released into fresh media, and fixed 8–9 hr later. Immunofluorescence of cells at defined stages of the cell cycle was performed with antibodies against Plk1 (left), phospho-T766 Gravin (middle, left), DNA (middle, right), and composite images (right).

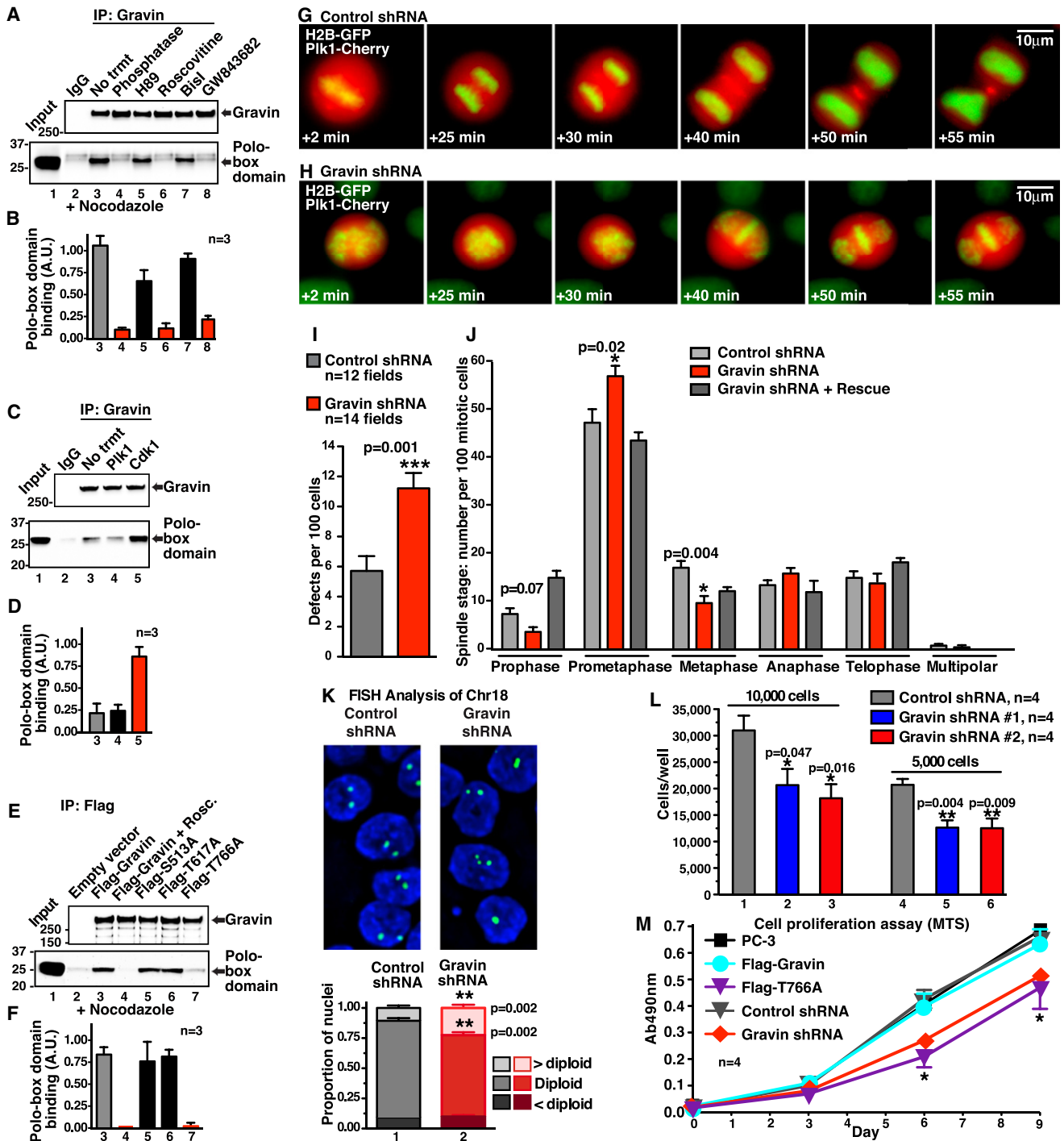


Figure 5. Gravin-Plk1 Interaction Facilitates Cell-Cycle Progression

(A) Mitotic HEK293 cells were treated for 4 hr with H89 (10 µM), Roscovitine (75 µM), Bisindolylmaleimide-1 (100 nM), or GW843682 (10 µM). Gravin immune complexes from each treatment (indicated above each lane) were incubated with a purified recombinant PBD fragment of Plk1 (371–603 aa). PBD-binding was assessed by immunoblot.

(B) Quantitation of the data shown in (A) (n = 3 ± SEM).

(C) Gravin immune complexes phosphorylated with Plk1 or CDK1/Cyclin B1 were assessed for binding to the recombinant PBD fragment.

(D) Quantitation of the data in (C) (n = 3 ± SEM).

(E) Flag-tagged Gravin or phosphosite mutants (indicated above each lane) were immunoprecipitated from mitotic cell lysates and incubated with recombinant PBD. Immunoblot detection of Gravin (top) and the PBD fragment (bottom) is shown.

(F) Quantitation of the data shown in (E) (n = 3 ± SEM).

On the basis of these biochemical results, we hypothesized that loss of Gravin or overexpression of the T766A mutant would have deleterious effects on mitosis and cell proliferation. We initially tested this hypothesis by visualizing the mitotic progression of HeLa cells upon gene silencing of Gravin. Cells that stably expressed control or Gravin shRNAs were released from a double-thymidine block and imaged every 20 s postrelease for 1 hr. Real-time fluorescent detection of Histone 2B-GFP monitored the position of chromatin, and imaging of Plk1-Cherry tracked the movement of the kinase. The majority of cells expressing control shRNA successfully completed mitosis (Figure 5G and Movie S1). Conversely, depletion of Gravin enhanced the incidence of mitotic defects (Figure 5H and Movie S2). Cells failed to successfully form a metaphase plate, often failing to divide or forming multinucleated daughter cells. These mitotic defects were scored per 100 cells over a longer time course (every 20 min for 12 hr; Movie S3 and Movie S4). A defect rate of $5.71\% \pm 0.98\%$ was recorded in cells stably expressing the control shRNA (Figure 5I; $n = 12$ fields). However, upon gene silencing of Gravin, the incidence of mitotic defects doubled to $11.21\% \pm 1.02\%$ (Figure 5I; $n = 14$ fields).

We performed a spindle-stage profile on these cells in order to identify the mitotic phase(s) where knockdown cells were stalling (Figure 5J). Cells depleted of Gravin progressed more rapidly through prophase, were delayed in prometaphase, and spent proportionally less time in metaphase as compared to shRNA controls (Figure 5J, light gray and red bars). Importantly, expression of an RNAi-resistant Gravin rescued the prophase and prometaphase defects (Figure 5J, dark gray bars, and Figure S5F). These results are consistent with the live-cell imaging data and provide context for the *in vivo* findings in Figure 1.

Next we evaluated genomic integrity following Gravin knockdown by fluorescence in situ hybridization using a probe against chromosome 18 (Figure 5K). Depletion of Gravin in near-diploid Hct116 cells led to a 2.13-fold increase in nuclei scored as “greater than diploid” compared to cells expressing control shRNA (Figure 5K, 0.106 ± 0.021 control shRNA (light gray bar) versus 0.226 ± 0.026 Gravin shRNA (pink bar); mean \pm SEM). Thus, loss of Gravin contributes to tetraploidy/aneuploidy.

Since knockdown of Gravin arrests cells in prometaphase, we asked whether depletion of the anchoring protein impacted cell proliferation. First, we performed colony-formation assays on PC-3 cells transfected with control shRNA or two shRNAs targeting Gravin (Figure 5L and Figure S5G). After 6 days of growth in soft agar, cell proliferation was analyzed using a cell transformation assay (Cell Biolabs). Depletion of Gravin with both shRNAs significantly reduced cell proliferation compared

to shRNA controls (Figure 5L, 33.33% and 41.33% decreases for shRNA #1 and #2 plated at 10,000 cells; 37.41% and 39.55% decreases at 5,000 cells; $n = 4 \pm$ SEM). Next, we monitored the impact of the Gravin T766A mutant on cell proliferation (Figure 5M). Parental PC-3 cells and cells stably expressing similar amounts of Flag-Gravin or Flag-T766A were plated in 96-well dishes and analyzed every 3 days by an MTS assay (Promega) as a surrogate for proliferation. Overexpression of Gravin did not affect the growth rates of cells compared to the parental line (Figure 5M, black and blue lines; $n = 4$). In contrast, the Gravin T766A mutant significantly decreased cell proliferation over the same time course (Figure 5M, purple line; $n = 4$). Moreover, shRNA-mediated knockdown of Gravin also decreased cell proliferation in this assay (Figure 5M, red and gray lines; $n = 4$). Introduction of charged aspartic and glutamic acid residues at T766 did not augment cell proliferation (Figure S5H). The data in Figure 5 infer that loss of Gravin increases mitotic defects and aneuploidy, and that both knockdown of Gravin and overexpression of a T766A phosphosite mutant that is unable to interact with Plk1 negatively impact cell proliferation.

Phospho-T766 Gravin and Glioblastoma Multiforme

Since disruption of the Plk1-Gravin interaction affects mitotic progression and cell proliferation, we reasoned that the phosphorylation state of Thr766 on Gravin could be a diagnostic marker for malignant neoplasms. Biochemical support for this concept was provided by evaluation of autopsied brain tissue from a patient afflicted with glioblastoma multiforme (a malignant, high-grade astrocytic neoplasm) that arose in the right parietal lobe of the brain (Figure 6A). Tumor tissue (confirmed histologically) was taken from the right lateral thalamus where there was dense glioblastoma infiltration without necrosis (Figure 6A, white box, left side). Histologically confirmed control samples were collected from the left temporal cortex (Figure 6A, white box, right side). Quantitative PCR demonstrated that Gravin mRNA was decreased $60.41\% \pm 3.88\%$ relative to a GAPDH control in these samples (Figure 6B). Conversely, and in keeping with our postulate, the phospho-T766 signal was elevated in Gravin immune complexes isolated from the tumor region when compared to normal tissue (Figure 6C, top panel, lanes 2 and 4).

We extended these findings by comparing cortical sections from glioblastoma resection specimens with age- and sex-matched control (nonneoplastic) cortical sections from patients who underwent lobectomy for surgical management of epilepsy. Magnetic resonance imaging (MRI) displayed no detectable

(G and H) HeLa cells stably expressing Histone 2B-GFP (green) and selected for stable incorporation of control or Gravin shRNAs were transfected with Plk1-Cherry (red). Montage of 63 \times images at defined times (indicated in each panel) after the cells were released from a double thymidine block.

(I) The number of mitotic defects was scored per 100 cells (Control shRNA, $n = 12$ fields; Gravin shRNA, $n = 14$ fields; mean \pm SEM).

(J) Spindle stage profile of HeLa cells expressing control shRNA (light gray; $n = 800 \pm$ SEM), Gravin shRNA (red; $n = 600 \pm$ SEM), or Gravin shRNA rescued with Gravin-mCherry (dark gray; $n = 500 \pm$ SEM).

(K) Fluorescence in situ hybridization of Hct116 cells transfected with control and Gravin shRNA. Nuclei were scored as greater than diploid, diploid, and less than diploid using a probe against chromosome 18 ($n = 10$ fields, >700 nuclei; representative images shown).

(L) Soft agar proliferation assay of prostate cancer (PC-3) cells (plated at 10,000 and 5,000 cells in 96-well dishes) expressing control or two independent Gravin shRNAs. Final cells number was analyzed after 6 days using a CyQuant green standard curve (Cell Biolabs; $n = 4 \pm$ SEM).

(M) Stable PC-3 cell lines were generated expressing Flag-Gravin or Flag-T766A, or transiently transfected with control or Gravin shRNA. Cells were plated in 96-well dishes, and proliferation was analyzed every 3 days by an MTS assay ($n = 4 \pm$ SEM, quadruplicate determinations; * $p \leq 0.05$).

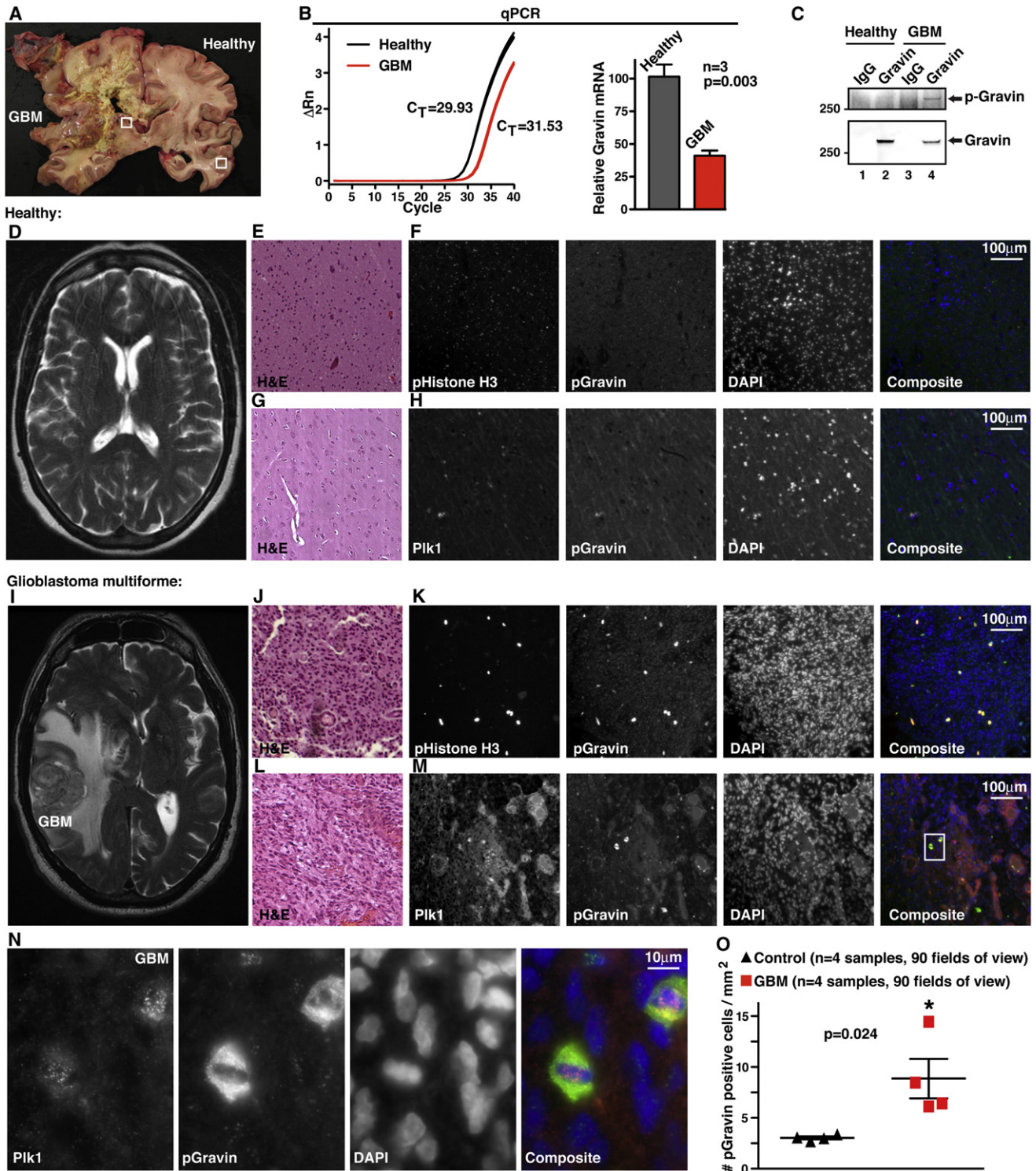


Figure 6. Phospho-T766 Gravin and Glioblastoma Multiforme

(A) Sagittal section of a brain collected during autopsy exhibiting glioblastoma multiforme (GBM) in the right parietal lobe. (B) Quantitative PCR of Gravin mRNA performed on tissue (white boxes) extracted from the GBM and uninvolved (“healthy”) contralateral side of the brain. Representative C_t trace (left) and Gravin mRNA levels normalized to GAPDH (right), $n = 3 \pm$ SEM. (C) Control (IgG) or Gravin immunoprecipitations were performed on brain extracts and probed for reactivity with phospho-T766 Gravin antisera. (D) Magnetic resonance imaging (MRI) of a healthy brain. (E and G) Paraffin-embedded sections of healthy brain tissue stained with H&E. (F) Serial sections costained with antibodies against phospho-S10 Histone H3, phospho-T766 Gravin, and DAPI followed by detection with secondary antibodies conjugated to Alexa Fluor dyes. (H) Additional sections costained with antibodies against Plk1, phospho-T766 Gravin, and DAPI.

lesions in the control brain (Figure 6D). H&E staining of paraffin-embedded sections from a temporal lobectomy specimen from this patient revealed normal six-layered cortex with reactive astrocytes and no hypercellularity or neoplasia (Figures 6E and 6G, Figure S6A). Weak staining for phospho-Histone H3 (red) in serial sections was consistent with a low mitotic index of the tissue (Figure 6F). Likewise, little phospho-T766 Gravin staining (green) was evident (Figure 6F). Nuclei were stained with the DNA marker DAPI (blue, Figure 6F). Similar results were obtained in serial sections stained with anti-Plk1 and phospho-T766 Gravin (Figure 6H).

Tumor sections were obtained from a patient with glioblastoma involving the right hemisphere (MRI in Figure 6I). H&E staining of the resected glioblastoma from this case showed a mitotically active, hypercellular, infiltrative astrocytic neoplasm with microvascular proliferation and pseudopalisading necrosis, confirming the glioblastoma diagnosis (Figures 6J and 6L, Figure S6B). Immunofluorescent detection of serial sections for phospho-Histone H3 and phospho-T766 Gravin revealed a preponderance of double positive cells (Figure 6K). This is indicative of increased mitosis within the tumor. Also, more Plk1 and phospho-T766 Gravin costaining was evident within the neoplasm (Figure 6M). At higher magnification, the phospho-T766 Gravin signal is concentrated at the mitotic spindle in two dividing cells (Figure 6N). This signal partially overlaps with Plk1, although a significant proportion of the enzyme decorates the kinetochores (Figure 6N). Quantitative analysis of sections from four patients with glioblastomas indicated a 3.0-fold increase in phospho-T766 Gravin compared to comparable regions of control brains (Figure 6O, 8.71 ± 1.93 cells/mm² in glioblastoma compared to 2.91 ± 0.14 cells/mm² in control; $n = 3 \pm$ SEM). The data in Figure 6 raise the possibility that phospho-T766 Gravin detection could be developed as a clinical biomarker or companion diagnostic for malignant neoplasms and other cancers.

DISCUSSION

The kinase anchoring protein Gravin has been designated as a tumor suppressor because the human gene resides in the q24-25.2 locus of chromosome 6, a deletion hotspot in advanced prostate, breast, and ovarian cancers (Xia et al., 2001). In addition, overexpression of the murine ortholog SSeCKS protects against anoikis in *v-Src*-transformed fibroblasts (Lin et al., 1996). Although both observations insinuate that Gravin might repress tumor growth, a growing body of evidence calls into question whether Gravin constitutes a bona fide tumor suppressor. For example, SSecks null mice are viable, and while they exhibit benign prostatic hyperplasia, they do not develop tumors (Akakura et al., 2008). Furthermore, gene array and proteomic analyses show that Gravin is upregulated in several transformed cell lines and cancers including chronic myeloge-

nous leukemia, bladder cancer, and follicular lymphomas (Jiang et al., 1997; Tsujimoto et al., 2005; Zhu et al., 2002). In this report we define an alternate role for Gravin in the spatial and temporal organization of phosphorylation-dependent protein-protein interactions that sustain mitosis. Several lines of evidence support this claim. While gene silencing of Gravin modestly increases tumor growth in immunodeficient mice, a more important consideration is that Gravin-depleted tumors have an elevated mitotic index. This may occur because Gravin depletion causes cells to stall during mitosis. This latter notion tallies with live-cell imaging and spindle profile studies that detect a prometaphase stall upon shRNA knockdown of Gravin in HeLa cells. Importantly, re-expression of Gravin rescued this defect. Thus, rather than solely exerting a dampening effect on mitosis, we propose that Gravin may augment the fidelity and reproducibility of cell division.

Protein phosphorylation by cyclin-dependent kinases (CDKs) drives eukaryotic cell division (Vermeulen et al., 2003). Our mass spectrometry analysis establishes that Gravin is phosphorylated at numerous sites during mitosis. Deeper biochemical analyses reveal that CDK1 phosphorylation of Thr766 on Gravin earmarks a subpopulation of the scaffolding protein for a specialized role in cell division via the recruitment of Plk1. A defining characteristic of Plk1 is the ability to transiently associate with different mitotic structures as cells progress through mitosis (Petronczki et al., 2008). Through mechanisms that are incompletely understood, these synchronized movements proceed through a C-terminal phosphopeptide-binding PBD that directs Plk1 toward its substrates and binding partners (Elia et al., 2003). Our findings argue that phospho-T766 Gravin participates in the sequestering of Plk1. However, depletion of Gravin was not found to substantially affect the localization of Plk1 (Figures S5I–S5R).

Immunofluorescence analysis in HEK293 and Rat-2 cells reveals that Gravin and Plk1 transiently associate during the early stages of mitosis. Both proteins are intermingled with DNA at prophase. This location is consistent with reports that Plk1 activity is necessary for chromosomal segregation (Jeong et al., 2010). Live-cell imaging experiments show that gene silencing of Gravin correlates with a higher incidence of mitotic abnormalities. These include protracted prometaphase, misalignment of chromosomes on the metaphase plate, and an increased prevalence of aneuploidy. Interestingly, analogous patterns of prometaphase arrest and the initiation of spindle assembly checkpoints are observed in cells treated with the Plk1 selective inhibitor BI2536 (Brennan et al., 2007; Petronczki et al., 2007). Likewise, elegant chemical-genetic approaches that acutely inactivate the kinase at the metaphase-to-anaphase transition show that Plk1 activity is necessary to initiate cytokinesis, a process that completes cell division to yield two physically distinct daughter cells (Burkard et al., 2007, 2009). Ancillary support for this latter scenario is highlighted by data showing

(I) Magnetic resonance imaging of a glioblastoma localized to the right hemisphere. (J and L) Paraffin-embedded sections of glioblastoma tissue stained with H&E. (K) Equivalent sections costained with antibodies against phospho-S10 Histone H3, phospho-T766 Gravin, and DAPI. (M) GBM sections costained with antibodies against Plk1, phospho-T766 Gravin, and DAPI. (N) The region in (M) indicated by the white box was imaged at higher magnification to visualize costaining of Plk1, phospho-T766 Gravin, and DAPI in mitotic tumor cells. (O) Quantitation of phospho-T766 Gravin-positive cells (per mm²) in sections from control and glioblastoma patients (Control patients, $n = 4$, 90 fields of view \pm SEM; GBM patients $n = 4$, 90 fields of view \pm SEM; $p = 0.024$).

that phospho-T766 Gravin staining remains at the centrosomes, whereas the Plk1 signal accumulates at the spindle midzone as cells enter anaphase. The segregation of these signals at later stages of mitosis not only emphasizes the precise temporal control that surrounds the Gravin-Plk1 interaction but also illustrates the remarkable mobility of this mitotic kinase. Thus, transient association with phospho-T766 Gravin offers a previously unrecognized means to direct Plk1 activity during the early phases of mitosis. Conversely, loss of this protein-protein interaction is deleterious to mitotic progression, as depletion of Gravin or overexpression of the nonphosphorylatable Gravin T766A mutant retards cell growth.

Grade 4 astrocytomas, more commonly known as glioblastomas, are extremely aggressive brain tumors (Van Meir et al., 2010). The median survival time from diagnosis is approximately 12 months, and standard treatment (surgery, radiotherapy, chemotherapy, and antiangiogenic drugs) only extends life expectancy by 5–7 months (Krex et al., 2007). Therefore the development of new prognostic markers for glioblastoma is critical. We show that phospho-T766 Gravin antiserum identifies rapidly dividing cells in paraffin-embedded sections from resected glioblastomas. Plk1 mRNA levels also increase in glioblastoma and correlate with both tumor classification and the probability of tumor recurrence after therapeutic intervention (Cheng et al., 2012). Thus, detection of the Gravin-Plk1 complex may have prognostic value; however, evaluation of many more clinical samples will be necessary to firmly establish this postulate. In conclusion, our discovery of this dynamic kinase-anchoring event underscores the exquisite molecular constraints required for cell-cycle progression. Moreover, our histological evaluation of phospho-T766 Gravin and Plk1 in clinical samples and dividing tumor cells leads us to speculate that aberrant control of this transient scaffolding event may have pathological ramifications.

EXPERIMENTAL PROCEDURES

Experimental Animals and In Vivo Tumorigenesis

U251 cells were injected subcutaneously into mice homozygous for *Foxn1^{nu}*. Tumor volume was measured from days 16 to 40. The institutional IACUC review committee approved all procedures used in this manuscript.

Cell Culture, Transfection, and Generation of Stable Cell Lines

Cells were maintained in DMEM or RPMI supplemented with 10% FBS and 1% penicillin/streptomycin (Invitrogen). Infections were performed with shRNA lentiviral particles (Santa Cruz Biotech). Transient transfections were performed using *TransIT-LT1* reagent (Mirus).

Immunoprecipitations and Tissue Analysis

Cells and tissue were homogenized in lysis buffer supplemented with protease and phosphatase inhibitors. Immunoprecipitations were rocked overnight with antibodies and protein A/G-agarose beads.

In Vitro Kinase Assays

Immunokinase assays were performed with 150 ng Plk1 or CDK1/Cyclin B1 (Cell Signaling Technology). Spindle prep kinase assays were performed with 300 μ M substrate peptide (ISDELMDATFADQEAKKK).

Immunofluorescence

Cells on coverslips were incubated overnight with primary antibodies, followed by detection with secondary antibodies conjugated to Alexa Fluor dyes

(Invitrogen). Imaging was performed on Zeiss 510 META confocal or Axio Observer.Z1 microscopes.

Statistical Analysis

All values are reported as mean \pm standard error (SEM), and the number of repeats (n) is shown on each figure. Statistical significance was determined by Student's t tests or ANOVA, with $p = 0.05$ as the significance level.

Patient Samples

The University of Washington Institutional Review Board approved the use of human samples in this study.

SUPPLEMENTAL INFORMATION

Supplemental Information includes six figures, one table, four movies, Supplemental Experimental Procedures, and Supplemental References and can be found with this article at <http://dx.doi.org/10.1016/j.molcel.2012.09.002>.

ACKNOWLEDGMENTS

This work was supported by NIH grants GM48231 (J.D.S.), GM69429 (L.W.), and DA14486 (N.S.); CIHR grant #MOP-6849 (T.P.); Canadian Cancer Society grant 019562 and Canada Research Chair (L.P.); and the Nancy and Buster Alvord Endowment (C.D.K.).

Received: January 24, 2012

Revised: July 5, 2012

Accepted: September 2, 2012

Published online: October 11, 2012

REFERENCES

- Ahn, N.G. (2009). PORE-ing over ERK substrates. *Nat. Struct. Mol. Biol.* *16*, 1004–1005.
- Akakura, S., Huang, C., Nelson, P.J., Foster, B., and Gelman, I.H. (2008). Loss of the *SSeCKS/Gravin/AKAP12* gene results in prostatic hyperplasia. *Cancer Res.* *68*, 5096–5103.
- Alexander, J., Lim, D., Joughin, B.A., Hegemann, B., Hutchins, J.R., Ehrenberger, T., Ivins, F., Sessa, F., Hudecz, O., Nigg, E.A., et al. (2011). Spatial exclusivity combined with positive and negative selection of phosphorylation motifs is the basis for context-dependent mitotic signaling. *Sci. Signal.* *4*, ra42. <http://dx.doi.org/10.1126/scisignal.2001796>.
- Bain, J., Plater, L., Elliott, M., Shpiro, N., Hastie, C.J., McLaughlan, H., Klevernic, I., Arthur, J.S., Alessi, D.R., and Cohen, P. (2007). The selectivity of protein kinase inhibitors: a further update. *Biochem. J.* *408*, 297–315.
- Brennan, I.M., Peters, U., Kapoor, T.M., and Straight, A.F. (2007). Polo-like kinase controls vertebrate spindle elongation and cytokinesis. *PLoS ONE* *2*, e409. <http://dx.doi.org/10.1371/journal.pone.0000409>.
- Burkard, M.E., Randall, C.L., Larochele, S., Zhang, C., Shokat, K.M., Fisher, R.P., and Jallepalli, P.V. (2007). Chemical genetics reveals the requirement for Polo-like kinase 1 activity in positioning RhoA and triggering cytokinesis in human cells. *Proc. Natl. Acad. Sci. USA* *104*, 4383–4388.
- Burkard, M.E., Maciejowski, J., Rodriguez-Bravo, V., Repka, M., Lowery, D.M., Clauser, K.R., Zhang, C., Shokat, K.M., Carr, S.A., Yaffe, M.B., and Jallepalli, P.V. (2009). Plk1 self-organization and priming phosphorylation of HsCYK-4 at the spindle midzone regulate the onset of division in human cells. *PLoS Biol.* *7*, e1000111. <http://dx.doi.org/10.1371/journal.pbio.1000111>.
- Cheng, M.W., Wang, B.C., Weng, Z.Q., and Zhu, X.W. (2012). Clinicopathological significance of Polo-like kinase 1 (PLK1) expression in human malignant glioma. *Acta Histochem.* *114*, 503–509.
- Christoph, D.C., and Schuler, M. (2011). Polo-like kinase 1 inhibitors in mono- and combination therapies: a new strategy for treating malignancies. *Expert Rev. Anticancer Ther.* *11*, 1115–1130.

- Dougherty, M.K., Ritt, D.A., Zhou, M., Specht, S.I., Monson, D.M., Veenstra, T.D., and Morrison, D.K. (2009). KSR2 is a calcineurin substrate that promotes ERK cascade activation in response to calcium signals. *Mol. Cell* 34, 652–662.
- Elia, A.E., Rellos, P., Haire, L.F., Chao, J.W., Ivins, F.J., Hoepker, K., Mohammad, D., Cantley, L.C., Smerdon, S.J., and Yaffe, M.B. (2003). The molecular basis for phosphodependent substrate targeting and regulation of Plks by the Polo-box domain. *Cell* 115, 83–95.
- Enserink, J.M., and Kolodner, R.D. (2010). An overview of Cdk1-controlled targets and processes. *Cell Div.* 5, 11.
- Fabbro, D., Cowan-Jacob, S.W., Möbitz, H., and Martiny-Baron, G. (2012). Targeting cancer with small-molecular-weight kinase inhibitors. *Methods Mol. Biol.* 795, 1–34.
- Gardino, A.K., and Yaffe, M.B. (2011). 14-3-3 proteins as signaling integration points for cell cycle control and apoptosis. *Semin. Cell Dev. Biol.* 22, 688–695.
- Gelman, I.H. (2010). Emerging roles for SSeCKS/Gravin/AKAP12 in the control of cell proliferation, cancer malignancy, and barrierogenesis. *Genes Cancer* 1, 1147–1156.
- Gordon, T., Grove, B., Loftus, J.C., O'Toole, T., McMillan, R., Lindstrom, J., and Ginsberg, M.H. (1992). Molecular cloning and preliminary characterization of a novel cytoplasmic antigen recognized by myasthenia gravis sera. *J. Clin. Invest.* 90, 992–999.
- Hoshi, N., Langeberg, L.K., Gould, C.M., Newton, A.C., and Scott, J.D. (2010). Interaction with AKAP79 modifies the cellular pharmacology of PKC. *Mol. Cell* 37, 541–550.
- Jeong, K., Jeong, J.Y., Lee, H.O., Choi, E., and Lee, H. (2010). Inhibition of Plk1 induces mitotic infidelity and embryonic growth defects in developing zebrafish embryos. *Dev. Biol.* 345, 34–48.
- Jiang, B.H., Agani, F., Passaniti, A., and Semenza, G.L. (1997). V-SRC induces expression of hypoxia-inducible factor 1 (HIF-1) and transcription of genes encoding vascular endothelial growth factor and enolase 1: involvement of HIF-1 in tumor progression. *Cancer Res.* 57, 5328–5335.
- Kolodner, R.D., Cleveland, D.W., and Putnam, C.D. (2011). Cancer. Aneuploidy drives a mutator phenotype in cancer. *Science* 333, 942–943.
- Krex, D., Klink, B., Hartmann, C., von Deimling, A., Pietsch, T., Simon, M., Sabel, M., Steinbach, J.P., Heese, O., Reifenberger, G., et al; German Glioma Network. (2007). Long-term survival with glioblastoma multiforme. *Brain* 130, 2596–2606.
- Lee, K.S., Park, J.E., Kang, Y.H., Zimmerman, W., Soung, N.K., Seong, Y.S., Kwak, S.J., and Erikson, R.L. (2008). Mechanisms of mammalian polo-like kinase 1 (Plk1) localization: self- versus non-self-priming. *Cell Cycle* 7, 141–145.
- Lin, X., and Gelman, I.H. (1997). Reexpression of the major protein kinase C substrate, SSeCKS, suppresses v-src-induced morphological transformation and tumorigenesis. *Cancer Res.* 57, 2304–2312.
- Lin, X., Tomblere, E., Nelson, P.J., Ross, M., and Gelman, I.H. (1996). A novel src- and ras-suppressed protein kinase C substrate associated with cytoskeletal architecture. *J. Biol. Chem.* 271, 28430–28438.
- Lowery, D.M., Clauser, K.R., Hjerrild, M., Lim, D., Alexander, J., Kishi, K., Ong, S.E., Gammeltoft, S., Carr, S.A., and Yaffe, M.B. (2007). Proteomic screen defines the Polo-box domain interactome and identifies Rock2 as a Plk1 substrate. *EMBO J.* 26, 2262–2273.
- Morrison, D.K., and Davis, R.J. (2003). Regulation of MAP kinase signaling modules by scaffold proteins in mammals. *Annu. Rev. Cell Dev. Biol.* 19, 91–118.
- Nauert, J.B., Klauck, T.M., Langeberg, L.K., and Scott, J.D. (1997). Gravin, an autoantigen recognized by serum from myasthenia gravis patients, is a kinase scaffold protein. *Curr. Biol.* 7, 52–62.
- Nihalani, D., Meyer, D., Pajni, S., and Holzman, L.B. (2001). Mixed lineage kinase-dependent JNK activation is governed by interactions of scaffold protein JIP with MAPK module components. *EMBO J.* 20, 3447–3458.
- Obenauer, J.C., Cantley, L.C., and Yaffe, M.B. (2003). Scansite 2.0: proteome-wide prediction of cell signaling interactions using short sequence motifs. *Nucleic Acids Res.* 31, 3635–3641.
- Petronczki, M., Glotzer, M., Kraut, N., and Peters, J.M. (2007). Polo-like kinase 1 triggers the initiation of cytokinesis in human cells by promoting recruitment of the RhoGEF Ect2 to the central spindle. *Dev. Cell* 12, 713–725.
- Petronczki, M., Lénárt, P., and Peters, J.M. (2008). Polo on the rise—from mitotic entry to cytokinesis with Plk1. *Dev. Cell* 14, 646–659.
- Scott, J.D., and Pawson, T. (2009). Cell signaling in space and time: where proteins come together and when they're apart. *Science* 326, 1220–1224.
- Silljé, H.H., and Nigg, E.A. (2006). Purification of mitotic spindles from cultured human cells. *Methods* 38, 25–28.
- Smith, F.D., Langeberg, L.K., Cellurale, C., Pawson, T., Morrison, D.K., Davis, R.J., and Scott, J.D. (2010). AKAP-Lbc enhances cyclic AMP control of the ERK1/2 cascade. *Nat. Cell Biol.* 12, 1242–1249.
- Strebhardt, K., and Ullrich, A. (2006). Targeting polo-like kinase 1 for cancer therapy. *Nat. Rev. Cancer* 6, 321–330.
- Tao, J., Wang, H.Y., and Malbon, C.C. (2003). Protein kinase A regulates AKAP250 (gravin) scaffold binding to the beta2-adrenergic receptor. *EMBO J.* 22, 6419–6429.
- Tsujimoto, K., Ono, T., Sato, M., Nishida, T., Oguma, T., and Tadakuma, T. (2005). Regulation of the expression of caspase-9 by the transcription factor activator protein-4 in glucocorticoid-induced apoptosis. *J. Biol. Chem.* 280, 27638–27644.
- Van Meir, E.G., Hadjipanayis, C.G., Norden, A.D., Shu, H.K., Wen, P.Y., and Olson, J.J. (2010). Exciting new advances in neuro-oncology: the avenue to a cure for malignant glioma. *CA Cancer J. Clin.* 60, 166–193.
- Vermeulen, K., Van Bockstaele, D.R., and Berneman, Z.N. (2003). The cell cycle: a review of regulation, deregulation and therapeutic targets in cancer. *Cell Prolif.* 36, 131–149.
- Willoughby, D., Wong, W., Schaack, J., Scott, J.D., and Cooper, D.M. (2006). An anchored PKA and PDE4 complex regulates subplasmalemmal cAMP dynamics. *EMBO J.* 25, 2051–2061.
- Xia, W., Unger, P., Miller, L., Nelson, J., and Gelman, I.H. (2001). The Src-suppressed C kinase substrate, SSeCKS, is a potential metastasis inhibitor in prostate cancer. *Cancer Res.* 61, 5644–5651.
- Zhu, Y., Hollmén, J., Rätty, R., Aalto, Y., Nagy, B., Elonen, E., Kere, J., Mannila, H., Franssila, K., and Knuutila, S. (2002). Investigatory and analytical approaches to differential gene expression profiling in mantle cell lymphoma. *Br. J. Haematol.* 119, 905–915.